European Heart Journal (2006) **27**, 1847–1854
doi:10.1093/eurheartj/ehl095

Ultrastructural evidence of intercalated disc remodelling in arrhythmogenic right ventricular cardiomyopathy: an electron microscopy investigation on endomyocardial biopsies

Cristina Basso[1], Elzbieta Czarnowska[2], Mila Della Barbera[1], Barbara Bauce[3], Giorgia Beffagna[4], Elzbieta K. Wlodarska[5], Kalliopi Pilichou[4], Angelo Ramondo[3], Alessandra Lorenzon[4], Olgierd Wozniek[5], Domenico Corrado[3], Luciano Daliento[3], Gian Antonio Danieli[4], Marialuisa Valente[1], Andrea Nava[3], Gaetano Thiene[1]*, and Alessandra Rampazzo[4]

[1] *Institute of Pathological Anatomy University of Padua, Italy;* [2] *Pathology Children's Memorial Health Institute, Warsaw, Poland;* [3] *Department of Cardiothoracic-Vascular Sciences, University of Padua, Italy;* [4] *Department of Biology, University of Padua, Italy; and* [5] *Institute of Cardiology, Warsaw, Poland*

Received 20 February 2006; revised 11 May 2006; accepted 26 May 2006; online publish-ahead-of-print 16 June 2006

KEYWORDS
Arrhythmogenic right ventricular cardiomyopathy;
Intercalated disc;
Myocyte;
Pathology;
Transmission electron microscopy;
Ultrastructure

Aims The ultrastructural features of the myocardium in arrhythmogenic right ventricular cardiomyopathy (ARVC) have not been systematically investigated so far. The recent discovery of gene mutations encoding intercalated disc proteins prompted us to perform a transmission electron microscopy study on endomyocardial biopsies.

Methods and results Twenty-one ARVC probands who fulfilled the international Task Force diagnostic criteria underwent right ventricular endomyocardial biopsy and screening of desmosome (D) protein encoding genes. Myocyte intercalated discs were analysed by transmission electron microscope and the data were compared with those of 10 controls and 10 patients with idiopathic dilated cardiomyopathy.

Extensive fibro-fatty replacement with a residual myocardium of 59 $\pm$ 23% was found in ARVC biopsy samples. Pathogenic D gene mutations were identified in 10 (48%): desmoglein-2 in four, desmoplakin in three and plakophilin-2 in three. Mean D length and D percent length of intercalated disc were significantly higher, D number was significantly lower and D gap was widened in ARVC. Moreover, abnormally located D in 75%, abnormal small junctions in 52%, and pale internal plaques in 32% of ARVC patients were found in the presence of a normal intercalated disc convolution index.

Conclusion The ultrastructural evidence of intercalated discs remodelling in ARVC, together with the positive screening of D protein encoding genes in half of probands, are in keeping with an intercellular junction cardiomyopathy.

Introduction

Arrhythmogenic right ventricular cardiomyopathy (ARVC) is a myocardial disease affecting the right ventricle, with or without left ventricular involvement, characterized by myocardial atrophy and progressive fibro-fatty tissue replacement accounting for life-threatening ventricular arrhythmias and sudden death.[1–4]

The disease is heredofamilial in up to 50% of cases[5] and six disease genes have been identified so far.[6–11] A deletion in plakoglobin has been proved to cause a recessive form of ARVC associated with palmoplantar keratosis and woolly hair, i.e. Naxos disease.[6] More recently, mutations of desmoplakin, plakophilin-2, and desmoglein-2 genes have been found in ARVC, in the absence of skin and hair abnormalities.[8,9,11] Plakoglobin, desmoplakin, plakophilin, and desmoglein are proteins of the intercellular junctions, i.e. fascia adherens (FA) and desmosome (D), that are responsible for the mechanical coupling of the myocytes and provide a continuous cell-to-cell connection to sarcomeric actin and intermediate filaments. These mechanical junctions are located, together with the electrical coupling nexus (or gap junction), at the bipolar ends of myocytes in the intercalated disc. As only little is known about the ultrastructure of the myocardium in ARVC, we undertook a transmission electron microscopic investigation of endomyocardial biopsies with special reference to intercalated disc morphology.

* Corresponding author: Institute of Pathological Anatomy University of Padua Medical School Via A. Gabelli, 61 35121 Padua, Italy. Tel: +39 049 8272283; fax: +39 049 8272284.
E-mail address: cardpath@unipd.it

Methods

ARVC patients were selected on the basis of: (i) a clinical diagnosis of ARVC according to the ISFC/ESC Task Force major and minor criteria;[12] (ii) quantitative histomorphometric criteria for ARVC at endomyocardial biopsy;[13] (iii) availability of an endomyocardial biopsy sample for transmission electron microscopy investigation.

Between 1985 and 2004, a total of 21 patients (10 males and 11 females, mean age 24.5 ± 14 years) retrospectively fulfilled the inclusion criteria. These patients underwent non-invasive and invasive screening at the Cardiology Division of the University of Padua, Padua, Italy ($n = 14$) and at the Institute of Cardiology, Warsaw, Poland ($n = 7$). Family history of ARVC was present in nine (43%). To assess the specificity of intercalated disc abnormalities in the time interval 2001–04, we prospectively collected a sample of endomyocardial biopsies for electron microscopy from 10 consecutive patients with a clinical diagnosis of idiopathic dilated cardiomyopathy (eight males and two females, mean age 38 ± 11, with a disease duration of at least 6 months, biventricular involvement and NYHA Class III and IV, and no evidence of fibro-fatty replacement at histology); and from 10 sex- and age-matched donor hearts (eight males and two females, mean age 40 ± 11) obtained before cardiac transplantation, who served as normal controls.

Histology

Right ventricular endomyocardial biopsy samples were obtained at the junction between the ventricular septum and the anterior right ventricular free wall via the femoral vein using the long sheath technique (disposable Cordis bioptome, Miami, FL, USA). Biopsy specimens were fixed in 10% phosphate-buffered formalin (pH 7.35) and processed for histologic examination. Seven-micron-thick paraffin-embedded sections were serially cut and stained by hematoxylin–eosin and Heidenhain trichrome.

The pathological diagnosis of ARVC was established on the basis of a significant amount of myocardial atrophy and fibro-fatty tissue replacement evaluated on samples stained with Heidenhain trichrome. Histomorphometric analysis was performed using an image analyser system and commercially available software (Image-Pro Plus Version 4.0) according to a previously described method.[13]

Transmission electron microscopy

Endomyocardial biopsy samples were routinely fixed in 2.5% glutaraldehyde in 0.1 M/L phosphate buffer (pH 7.3) and postfixed in buffered 1% osmium tetroxide for 1 h. Samples were then dehydrated in a series of ethanol and embedded in Epon 812. Semithin sections were first evaluated at light microscope before proceeding to ultrathin sections. Thin sections were stained with uranyl acetate and lead citrate and examined under a Hitachi H-7000 electron microscope equipped with digital camera. Before analysing electron micrographs, tissue sections were inspected to avoid contraction bands and artefactual changes. Myocyte nucleus, cytoplasmic organelles, lipid droplets, glycogen amount, and sarcolemma as well as interstitial space abnormalities were evaluated.

As far as intercalated discs are concerned, random fields of many longitudinally sectioned myocytes were analysed to obtain a total of 10 intercalated discs per patient. Intercalated discs were first photographed at low magnification to measure their total length, then all portions containing D, FA, and nexus were photographed again for further analysis at a final magnification of ×30000 and ×60000. By histomorphometric analysis system, the intercalated disc length was evaluated both as straight end-to-end distance and as real distance following its profile. Then, convolution index was expressed as the real distance of intercalated disc divided by the end-to-end distance. Moreover, D and nexus length (micron), D and nexus percent length of intercalated disc, D and nexus number per 10 μ unit length of intercalated disc, and D and FA gap size (nm) were calculated. All values are expressed as mean ± SD. Junctional changes, including both D and FA, were then evaluated.

Ultrastructural morphology was analysed by three independent observers (C.B., E.C., and M.D.B.) blinded to the clinical diagnosis.

Genetic analysis

ARVC patients were screened for desmoplakin, plakophilin-2, TGFbeta3, and desmoglein-2 mutations by denaturing high-performance liquid chromatography (DHPLC) and subsequent direct sequencing of amplicons showing abnormal elution profiles. Patients did not show either effort-induced polymorphic ventricular arrhythmias nor gross skin/hair abnormalities, thus mutation screening of RyR2 and plakoglobin was not performed. PCR amplifications were performed using standard protocols (Taq Gold, Applied Biosystems), as previously reported.[8–11] DHPLC analysis was performed using WAVE® Nucleic Acid Fragment Analysis System 3500HT with DNASep® HT cartridge (Transgenomic Ltd, NE, USA). Temperatures for sample analysis were selected using WAVEMAKER™ software. All amplimers showing a change in DHPLC pattern were sequenced using the BIG DYE dideoxy-terminator chemistry on an ABI 3730XL DNA sequencer (PE Applied Biosystems). Chromas 1.5 and LASERGENE (DNASTAR) softwares were used to edit, assemble, and translate DNA sequences. A control group of 100 healthy and unrelated subjects (200 alleles) from the same population was used to assess whether detected mutations were common DNA polymorphisms.

For further analysis of the splice site mutation c.542 + 5G>A in DSP gene, mRNA was isolated from 2.5 mL whole blood of the patient, using PAXgene™ Blood RNA kit (Qiagen) following the supplier protocol. The corresponding cDNA was obtained from an RT-PCR reaction using 1 μg total RNA. The following primers were used in the first round PCR to amplify the fragment corresponding to exons 1–4: 5′GGTAGCGAGCAGCGACCTC3′ and 5′CTCATCCACCCC AAACATTC3′. DSP cDNA product was re-amplified by using nested PCR oligonucleotides (5′GACCTGCGCTACGAGGTGA3′ and 5′CTGGG CAAAACACTCATCCA3′). The nested PCR product was directly sequenced.

Statistical analysis

Comparisons between the three groups were performed by analysis of variance (ANOVA) and Student's *t*-test. All continuous variables were expressed as the mean value ±1 SD for each measurement. Due to the small sample size and the different variabilities across the groups, a Mann–Whitney test for all possible combinations of mean pairs was also performed. All tests were two-tailed. To account for multicomparison problem and for increasing the type I error associated with the usage of multiple tests on the same data, we used a Bonferroni correction and thus, we considered only the *P*-values ($P \leq 0.016$) as statistically significant. Linear regression analysis (Pearson correlation) was used to correlate the ultrastructural parameters with age.

Results

Clinical findings

Main clinical features of ARVC patients are summarized in *Table 1*.

Histology

After informed consent, endomyocardial biopsy samples were obtained in each patient (mean 2.1 ± 0.7 samples per patient) for a mean biopsy area of 1.4 ± 0.6 mm^2.

At histomorphometric evaluation, the endomyocardial biopsy area consisted of 59 ± 23% myocardium, 21 ± 20% fibrous tissue, and 18 ± 17% fatty tissue. Myocyte

abnormalities, consisting of dysmetric and dysmorphic nuclei and cytoplasmic vacuolization, were observed in all.

Genetic study

Mutation screening of ARVC genes desmoplakin, plakophilin2, TGFbeta3, and desmoglein2 was performed in all 21 unrelated probands.

Pathogenic mutations were identified in 10 patients (48%): three of them resulted to carry a desmoplakin mutation (K470E, A566T, K1583R, c.542 + 5G>A), three a plakophilin-2 mutation (V587I, N670fs683X, Q707X), and four a desmoglein-2 mutation (G100R, E418fs419X, Q557X, E712K). In one patient, two different desmoplakin missense mutations (K470E and A556T) were found. No TGFbeta3 mutations were detected. None of the nucleotide changes were identified in 100 control subjects from the same population. All missense mutations occurred in residues highly conserved among species.

Table 1 Main clinical features in ARVC patients

	n	%
Male	10	48.0
Mean age (years)	24.5 ± 14	
Family history of ARVC	9	43.0
Syncope	4	19.0
ECG		
Inverted T-wave >V2	10	48.0
QRS >120 ms	8	38.0
LBBB ventricular arrhythmias	18	86.0
Positive SAECG	12	57.0
Two-dimensional echo		
RV aneurysms	11	52.0
RV dilatation	15	71.0
LV involvement	5	24.0
Therapy		
Implantable cardioverter defibrillator	4	19.0
Catheter ablation	2	9.5
Antiarrhythmic drug therapy	18	86.0

LBBB, left bundle branch block; LV, left ventricle; RV, right ventricle; SAECG, signal-averaged ECG.

Two nonsense mutations (Q707X in plakophilin-2 and Q557X in desmoglein-2) and two insertion–deletion mutations (N670fs683X in plakophilin-2 and E418fs419X in desmoglein-2) cause insertion of a premature stop codon, with consequent truncation of the C-terminal domains.

Mutation c.542 + 5G>A alters the donor splicing site of intron 2. After reverse transcription of lymphocytes RNA, DSP cDNA corresponding to exons 1–3 was nested–PCR amplified and sequenced. This analysis failed to detect aberrant transcripts and showed only the wild-type allele, suggesting that the aberrant transcripts would be degraded, most likely through nonsense-mediated mRNA decay.[14]

Transmission electron microscopy

Golgi apparatus, sarcoplasmic reticulum, and T-tubules abnormalities were never found in ARVC. Normally arranged myofibrils within the sarcomeres with defined Z-bands were visible in all ARVC cases. Lipofuscin deposits were seen in a similar amount in ARVC and controls. Polymorphic mitochondria were observed in six and irregular cristae in five ARVC cases vs. none of the controls.

Highly convoluted nuclei with dense aggregates of chromatin beneath the nuclear membrane were detected in all ARVC cases, and nuclear changes in keeping with apoptosis/early apoptosis were observed in five (24%). Microsteatosis with intracellular lipid droplets was detected in 18 (86%) and increased glycogen granules in all, while they were rarely observed in controls. Increased interstitial collagen and cellular debris were detected in all ARVC cases. Endothelial cell ultrastructural abnormalities were not observed.

Intercalated discs findings

Major findings are reported in *Table 2*. The mean D length, the D percent length of intercalated disc, the D gap, and the FA gap were significantly higher in ARVC than in controls, and both the D and nexus number per 10 μ unit length of intercalated disc were lower in ARVC than in controls (*Figures 1* and *2*). No difference was found in terms of convolution index. Moreover, the mean D length was higher and the D number per 10 μ unit length of intercalated disc was lower in ARVC than in dilated cardiomyopathy,

Table 2 Intercalated discs: morphometric ultrastructural findings

Intercalated disc	ARVC (21)	DC (10)	Controls (10)	*P*-value ARVC vs. controls	*P*-value ARVC vs. DC	*P*-value DC vs. controls
Convolution index	3.0 ± 0.9	2.8 ± 0.5	2.8 ± 0.6	0.34	0.18	0.76
D mean length (μm)	0.31 ± 0.08	0.23 ± 0.1	0.16 ± 0.08	<0.001	0.04	0.11
n, D/10 μm unit length	3.34 ± 0.9	4.2 ± 0.8	5.54 ± 2.3	0.01	0.02	0.10
D percent length of intercalated disc (%)	9.8 ± 3.2	8.4 ± 2.2	5.7 ± 1.4	<0.001	0.16	0.008
Nexus mean length (μm)	0.34 ± 0.15	0.31 ± 0.07	0.32 ± 0.16	0.78	0.47	0.69
n, Nexus/10 μm unit length	0.29 ± 0.86	0.23 ± 0.32	0.78 ± 0.54	0.03	0.64	0.02
Nexus percent length of intercalated disc (%)	1.2 ± 1.8	1.14 ± 1.5	3.0 ± 2.5	0.07	0.93	0.08
D mean gap (nm)	29.33 ± 8.95	24.21 ± 2.1	21.78 ± 3.42	0.004	0.03	0.19
FA mean gap (nm)	41.49 ± 20.36	28.39 ± 5.1	27.18 ± 10.72	0.03	0.02	0.67

DC, dilated cardiomyopathy.
After Bonferroni correction, only $P \leq 0.016$ are significant.

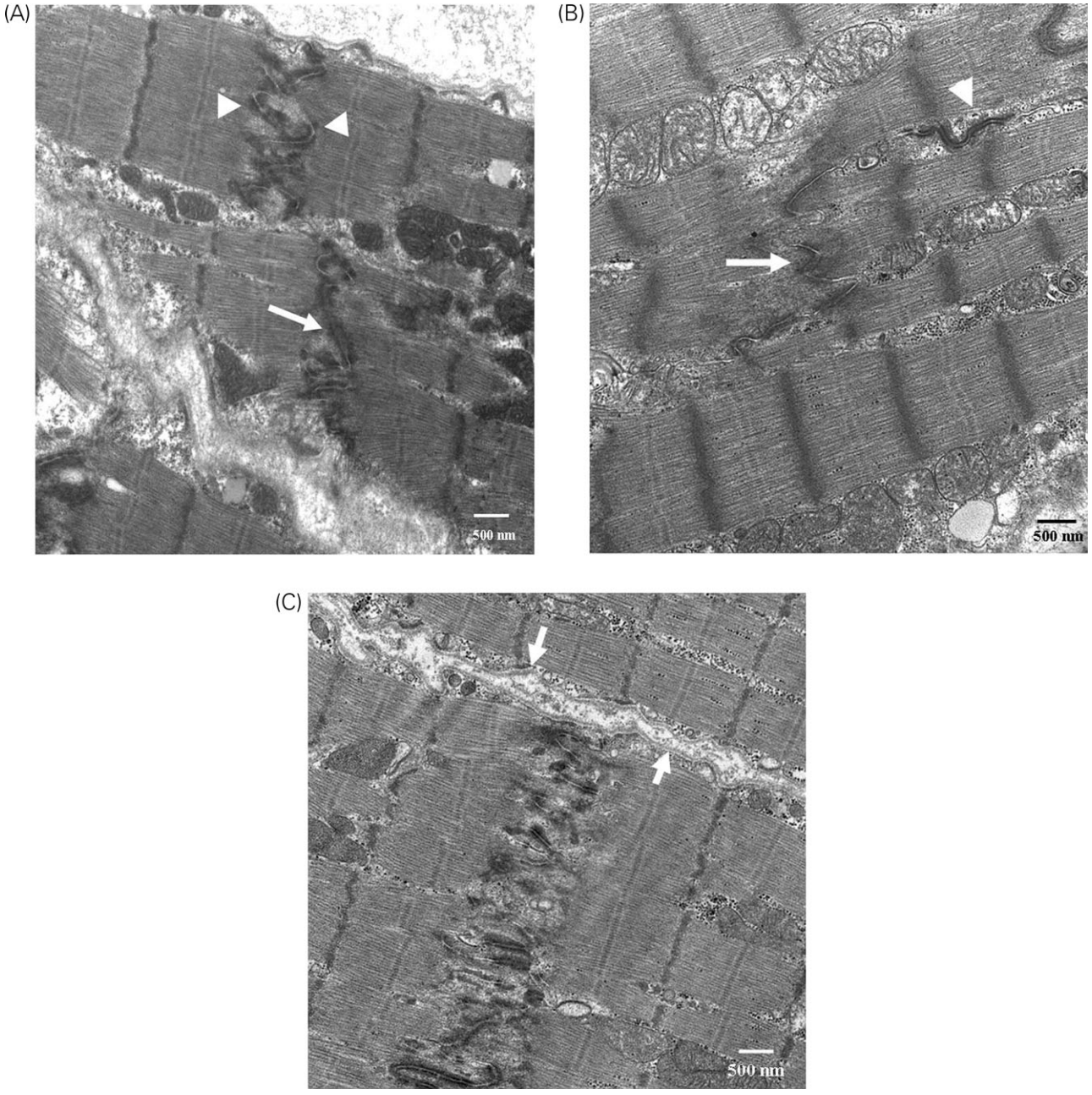

Figure 1 Panoramic view of cardiac myocyte intercalated discs. (*A*) ARVC patient who was negative at genetic screening. Widened gap of FA (arrow) and abnormal position of Ds at the level of myofilaments line (arrowheads) are visible. (*B*) ARVC patient with desmoplakin gene splice site mutation (c.542 + 5G>A). Note the abnormal position of long Ds (arrowhead) and the widened gap of FA (arrow). (*C*) Control case. Regular membrane (arrows) and intercalated disc between adjacent myocytes. Original magnification: ×15 000.

whereas no statistically significant difference was found when assessing the other parameters. ANOVA and Mann–Whitney tests were performed and have produced similar results.

Abnormal small junctions composed of series of repeating couplings were observed in 11 out of 21 ARVC cases (52%) (*Figure 2A*) and abnormally located Ds in 75% of ARVC but were never found in dilated cardiomyopathy and controls. Moreover, pale internal plaques were found in 32% of ARVC (*Figure 3*) and 30% of dilated cardiomyopathy vs. none of controls.

No statistically significant differences were found between genotype-positive (10 cases) and genotype-negative (11 cases) ARVC patients. In particular, the convolution index was 3.2 ± 1.1 vs. 3.06 ± 1.2 ($P = 0.9$), the D length 0.29 ± 0.08 vs. 0.27 ± 0.07 ($P = 0.6$), the D number per 10 μ unit length of intercalated disc 3.4 ± 0.8 vs. 3.6 ± 1.2 ($P = 0.8$), and the D gap 29,6 ± 12.4 vs. 27.3 ± 6.16 ($P = 0.6$).

By linear regression analysis, no correlation was found in ARVC cases between age and any of the D ultrastructural parameters investigated (convolution index $R^2 = 0.000335$, D mean length $R^2 = 0.0769$, D number per 10 μ unit length of intercalated disc $R^2 = 0.00612$, D percent length of intercalated disc $R^2 = 0.0117$, D mean gap $R^2 = 0.00556$).

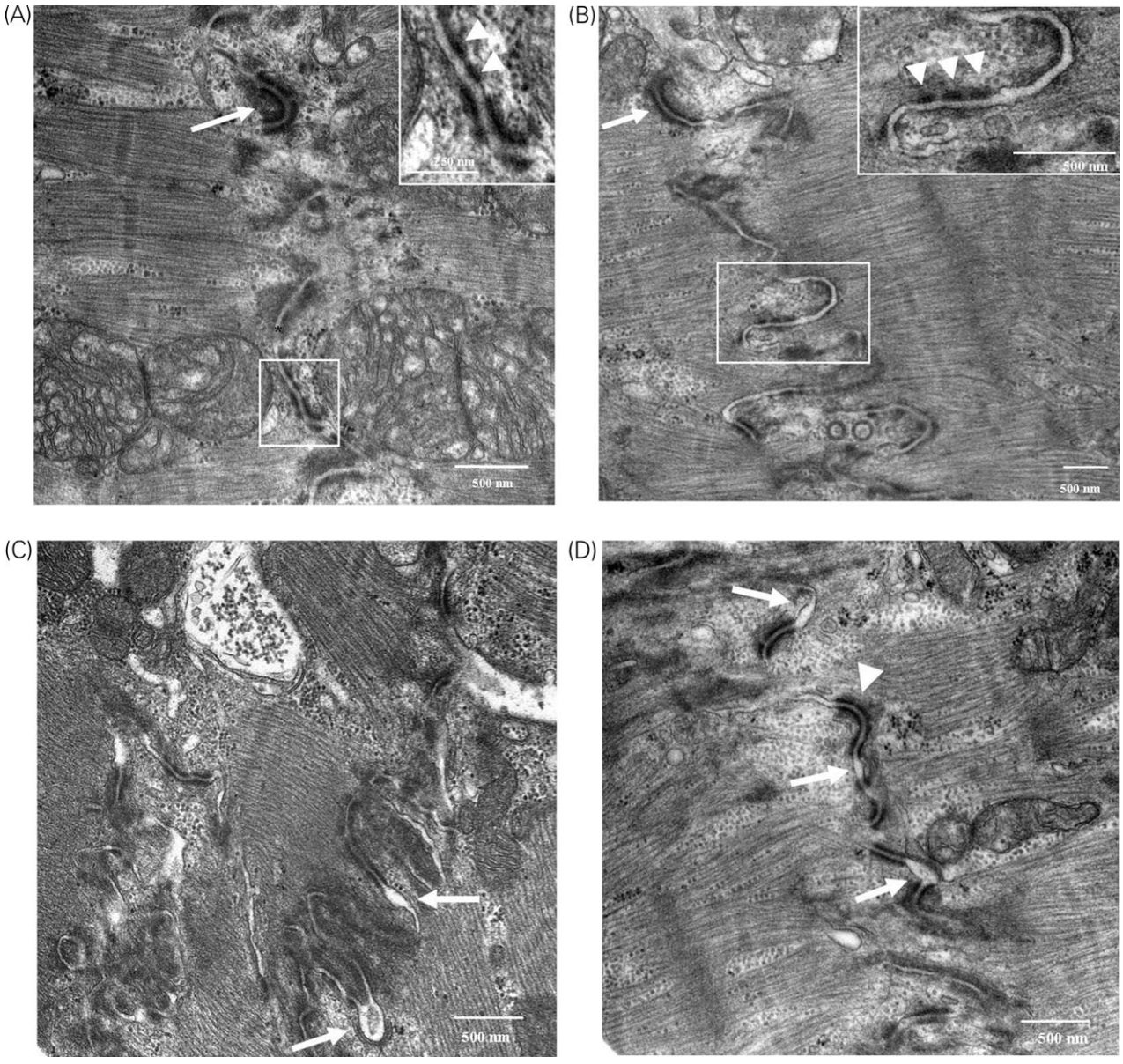

Figure 2 Mechanical junctions of intercalated discs in ARVC. (*A*) ARVC patient who was negative at genetic screening. Panoramic view of the pale intercalated disc junctions with long D (arrow) and series of short Ds. Nexus is not visible. In insert, close-up of repeating short Ds (arrowheads). Original magnification: ×15 000. (*B*) ARVC patient with desmoplakin gene mutation (K1583R). Panoramic view of the pale intercalated disc junctions showing the same features observed in A. In insert, close-up of repeating short Ds (arrowheads). Original magnification: ×15 000. (*C*) Same patient as *Figure 2A*. Segment of the intercalated disc exhibiting disarrangement of filaments and widening of FA gap (arrows). Original magnification: ×30 000. (*D*) Same patient as *Figure 2B*. Segment of the intercalated disc exhibiting long D (arrowhead), disarrangement of filaments, widening of FA gap (arrows), and abundant glycogen particles. Original magnification: ×30 000.

Discussion

Despite the amount of investigation on the morphologic aspects and on the aetiopathogenesis of ARVC, few investigators addressed the ultrastructural features so far. In this study, we first analysed by transmission electron microscopy and morphometric analysis a consecutive series of ARVC patients with a clear-cut clinical and histological diagnosis, providing evidence of highly convoluted nuclei, increased lipid droplets, and intercalated disc remodelling.

Intercalated discs and ARVC

Three types of intercellular junctions, i.e. D, FA, and nexus, exhibiting different functions and precise localization, provide the basis for the functional syncytium of cardiac muscle.[15–17] D accounts for the mechanical stability of cell-to-cell connections, while FA for the transmission of force developed by contracting myofibrils. The FA is formed by cadherins, i.e. calcium-dependent cell-to-cell adhesion molecules that are connected with the actin network in a complex with intracellular attachment proteins (α-, β-, γ- catenins, and others). The Ds show an electron-dense cytoplasmic plaque, comprising an outer plaque and an inner plaque, through which the intermediate filaments appear to loop. At this level, γ-catenin (i.e. plakoglobin) interacts with D cadherins, i.e. desmocollins and desmogleins, and with desmoplakin, which in turns binds to intermediate filaments. This D-intermediate filaments

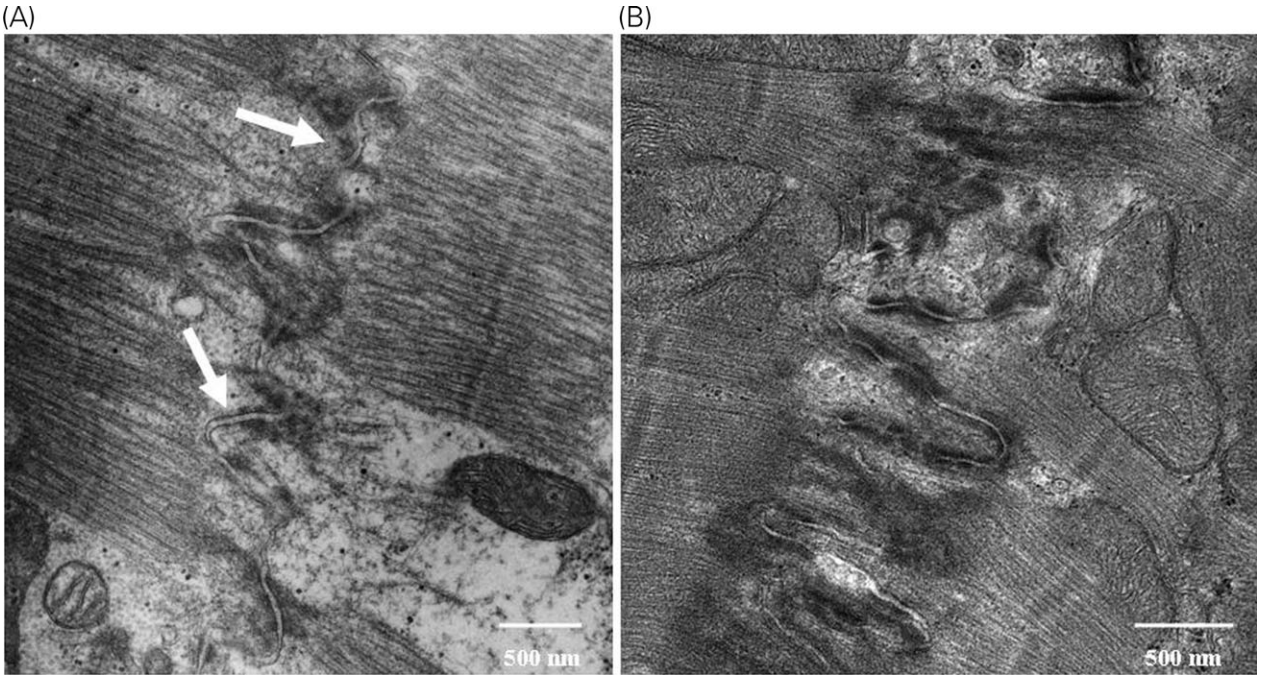

Figure 3 Paleness of D internal plaques (arrows) in ARVC (*A*) vs. control (*B*). Original magnification: ×30 000.

complex forms a continuous transcellular network of structural proteins that is crucial for maintaining the integrity of tissues and organs exposed to mechanical stress, such as the skin and the heart. Lack of normal communication between myocytes leads to functional injury. Although the abnormal distribution and expression of junctional proteins have been described in several myocardial diseases,[18–24] information concerning the intercalated disc structure in ARVC has been limited so far. The growing interest on intercellular junction follows the identification of a 2 bp deletion in plakoglobin in Naxos-ARVC and of desmoplakin, plakophilin-2,[6,8,9] and more recently of desmoglein-2[11] gene mutations in dominant ARVC, and the evidence that plakoglobin null-mutant mouse embryos show decreased myofibre compliance and reduced cell-to-cell adhesion as a consequence of defects in D number and structure.[25] Impairment of myocyte cell-to-cell adhesion has been advocated as a possible common pathway in ARVC. Failure of D to couple cells will inevitably lead to tissue and organ fragility. As with mutations in plakoglobin, defects in other D proteins could result in altered integrity at cardiac cell-to-cell junctions that is sufficient to promote myocyte death under stress conditions. Then, repair takes place through fibro-fatty replacement, providing the anatomical basis for life-threatening re-entry arrhythmias and progressive heart failure.

Other investigators previously explored the ultrastructural features of ARVC.[26,27] In particular, in 1989, Guiraudon[27] first showed that intercalated discs may present pale structure and flattened convolutions with rare or small D and decreased filaments in the area of FA, but few cases of ARVC were investigated and not quantitative data were provided. The loosening of all attachments with poor cohesion of the myocytes has been postulated to explain their dissociation with adipose tissue infiltration.[27] Our results confirm these preliminary findings, showing a substantial remodelling of intercalated discs in ARVC. Abnormal small junctions composed of series of repeating couplings and elongated D have been observed in ARVC, which are quite similar to those reported in Carvajal syndrome, a disease caused by a recessive mutation of desmoplakin,[28] but were never observed in dilated cardiomyopathy or in controls. Moreover, a decreased D number per unit tissue area was observed in ARVC and controls and D were often relocated in a wrong position, i.e. where the FA is usually placed in normal myocytes. The reason for this remodelling is not known and further genetic studies and immunohistochemical localization of cell-to-cell junction proteins are required. Note that the D gap was wider in ARVC than in dilated cardiomyopathy and controls. This could be an effect of abnormal expression of transmembrane proteins that establish intercellular contacts. At the cytoplasmic face, the intercalated discs are frequently pale both in ARVC and dilated cardiomyopathy, which might suggest an abnormal composition of proteins that bind cytoplasmic tails of β-catenin in the FA and cadherins in D. The absence of abnormal small junctions and abnormally located D in dilated cardiomyopathy supports the view that these features should be considered as a specific marker of ARVC. Whether these abnormalities would be present in concealed forms as an early diagnostic marker remains to be elucidated in prospective electron microscopy studies. At present, we cannot recommend electron microscopy for routine diagnostic purposes but only for research.

In nearly half of the cases, we found evidence of D proteins encoding gene mutations, i.e. desmoplakin, plakophilin-2, and desmoglein-2. In contrast, in the remaining genotype-negative ARVC cases, other still unknown disease-causing genes are likely to be involved. This could explain why D remodelling was present at ultrastructural level in both genetic-positive and genetic-negative ARVC

patients, as to support the view that many ARVC forms have to be considered as intercellular junction cardiomyopathies due to D proteins abnormalities.

As far as electrical coupling is concerned, a decreased nexus number has been found both in ARVC and dilated cardiomyopathy. It is noteworthy that remodelling of nexus has been already reported in Carvajal syndrome and in Naxos-ARVC.[22,29] The authors postulated that an abnormal linkage between mechanical junctions and the cytoskeleton might be directly responsible for gap junctions remodelling. Our data seem in keeping with the hypothesis that a similar remodelling of electrical junction occurs in ARVC and dilated cardiomyopathy.

Nuclear and cytoplasmatic abnormalities in ARVC

Convoluted nuclei, similar to those recently described by Runge *et al.*[30] and interpreted as an early expression of apoptosis, have been observed in the majority of our ARVC patients. We previously demonstrated the occurrence of myocyte apoptosis in more than one-third of ARVC cases on endomyocardial biopsy by applying both transmission electron microscopy and TUNEL.[31] As plakoglobin can also act as a signalling molecule by the induction of anti-apoptotic protein Bcl-2,[32] further studies are required to establish the link between cell-to-cell junctions and intracellular signalling pathways.

Apart from the exceptional reports of mitochondrial abnormalities,[33] a lot of attention has been paid on intracellular lipid droplets,[34,35] which were present in the majority of our ARVC cases. The presence of multiple sarcoplasmic vacuoles of lipidic nature in cardiac myocytes, mostly replacing the myofibril component, has been interpreted as a possible marker of myocyte transdifferentiation into adipocytes.[36]

Conclusions

ARVC is characterized by intercalated discs ultrastructural abnormalities consisting of decreased D number and increased D length, pale D and abnormal small junctions, and intercellular gap widening in the absence of convolution. These ultrastructural features, together with the demonstration of D protein encoding genes mutations in half of the cases, are strongly in keeping with a cell-to-cell junction cardiomyopathy.[37]

Acknowledgements

This study was supported by Ministry of Health, MURST and Telethon Grant GGP05261, Rome; Fondazione Cassa di Risparmio, Padova e Rovigo; ARVC/D Project, QLG1-CT-2000-01091 Fifth Framework Programme European Commission, Bruxelles. The authors are deeply indebted to Chiara Romualdi for statistical analysis support.

Conflict of interest: none declared.

References

1. Nava A, Rossi L, Thiene G. *Arrhythmogenic Right Ventricular Cardiomyopathy/Dysplasia*. Amsterdam: Elsevier Science B.V., 1997.
2. Marcus FI, Fontaine GH, Guirardon G, Frank R, Laurenceau JL, Malergue C, Grosgogeat Y. Right ventricular dysplasia: a report of 24 adult cases. *Circulation* 1982;**65**:384–398.
3. Thiene G, Nava A, Corrado D, Rossi L, Pennelli N. Right ventricular cardiomyopathy and sudden death in young people. *N Engl J Med* 1988;**318**:129–133.
4. Basso C, Thiene G, Corrado D, Angelini A, Nava A, Valente M. Arrhythmogenic right ventricular cardiomyopathy. Dysplasia, dystrophy or myocarditis? *Circulation* 1996;**94**:983–991.
5. Nava A, Bauce B, Basso C, Muriago M, Rampazzo A, Villanova C, Daliento L, Buja G, Corrado D, Danieli GA, Thiene G. Clinical profile and long term follow-up of 37 families with arrhythmogenic right ventricular cardiomyopathy. *J Am Coll Cardiol* 2000;**36**:2226–2233.
6. McKoy G, Protonotarios N, Crosby A, Tsatsopoulou A, Anastasakis A, Coonar A, Norman M, Baboonian C, Jeffery S, McKenna WJ. Identification of a deletion in plakoglobin in arrhythmogenic right ventricular cardiomyopathy with palmoplantar keratoderma and woolly hair (Naxos disease). *Lancet* 2000;**355**:2119–2124.
7. Tiso N, Stephan DA, Nava A, Bagattin A, Devaney JM, Stanchi F, Larderet G, Brahmbhatt B, Brown K, Bauce B, Muriago M, Basso C, Thiene G, Danieli GA, Rampazzo A. Identification of mutations in the cardiac ryanodine receptor gene in families affected with arrhythmogenic right ventricular cardiomyopathy type 2 (ARVD2). *Hum Mol Genet* 2001;**10**:189–194.
8. Rampazzo A, Nava A, Malacrida S, Beffagna G, Bauce B, Rossi V, Zimbello R, Simionati B, Basso C, Thiene G, Towbin JA, Danieli GA. Mutation in human desmoplakin domain binding to plakoglobin causes a dominant form of arrhythmogenic right ventricular cardiomyopathy. *Am J Hum Genet* 2002;**71**:1200–1206.
9. Gerull B, Heuser A, Wichter T, Paul M, Basson CT, McDermott DA, Lerman BB, Markowitz SM, Ellinor PT, MacRae CA, Peters S, Grossmann KS, Drenckhahn J, Michely B, Sasse-Klaassen S, Birchmeier W, Dietz R, Breithardt G, Schulze-Bahr E, Thierfelder L. Mutations in the desmosomal protein plakophilin-2 are common in arrhythmogenic right ventricular cardiomyopathy. *Nat Genet* 2004;**36**:1162–1164.
10. Beffagna G, Occhi G, Nava A, Vitiello L, Ditadi A, Basso C, Bauce B, Carraro G, Thiene G, Towbin JA, Danieli GA, Rampazzo A. Regulatory mutations in transforming growth factor-β3 gene cause arrhythmogenic right ventricular cardiomyopathy type 1. *Cardiovasc Res* 2005;**65**:366–373.
11. Pilichou K, Nava A, Basso C, Beffagna G, Bauce B, Lorenzon A, Frigo G, Vettori A, Valente M, Towbin J, Thiene G, Danieli GA, Rampazzo A. Mutations in Desmoglein-2 gene are associated to arrhythmogenic right ventricular cardiomyopathy. *Circulation* 2006;**113**:1171–1179.
12. McKenna WJ, Thiene G, Nava A, Fontaliran F, Blomstrom-Lundqvist C, Fontaine G, Camerini F. Diagnosis of arrhythmogenic right ventricular dysplasia/ cardiomyopathy. *Br Heart J* 1994;**71**:215–218.
13. Angelini A, Basso C, Nava A, Thiene G. Endomyocardial biopsy in arrhythmogenic right ventricular cardiomyopathy. *Am Heart J* 1996;**132**:203–206.
14. Maquat LE, Carmichael GG. Quality control of mRNA function. *Cell* 2001;**104**:173–176.
15. Langer GA. The structure and function of the myocardial cell surface. *Am J Physiol* 1978;**235**:H461–H468.
16. Forbes MS, Sperelakis MS. Intercalated discs of mammalian heart: a review of structure and function. *Tissue and cell* 1985;**17**:605–648.
17. Severs NJ. The cardiac gap junction and intercalated disc. *Int J Cardiol* 1990;**26**:137–173.
18. Fujio Y, Yamada-Honda F, Sato N, Funai H, Wada A, Awata N, Shibata N. Disruption of cell-cell adhesion in an inbred strain of hereditary cardiomyopathic hamster (Bio 14. 6). *Cardiovasc Res* 1995;**30**:899–904.
19. Schaper J, Froede R, Hein S, Buck A, Hashizume H, Speiser B, Friedl A, Bleese N. Impairment of the myocardial ultrastructure and changes of the cytoskeleton in dilated cardiomyopathy. *Circulation* 1991;**83**:504–514.
20. Peters NS, Green CR, Poole-Wilson PA, Severs NJ. Reduced content of connexin43 gap junctions in ventricular myocardium from hypertrophied and ischaemic human hearts. *Circulation* 1993;**88**:864–875.
21. Wang X, Gerdes AM. Chronic pressure overload cardiac hypertrophy and failure in guinea pigs: III. Intercalated disc remodeling. *J Mol Cell Cardiol* 1999;**31**:333–343.
22. Kaplan SR, Gard JJ, Carvajal-Huerta L, Ruiz-Cabezas JC, Thiene G, Saffitz JE. Structural and molecular pathology of the heart in Carvajal syndrome. *Cardiovasc Pathol* 2004;**13**:26–32.
23. Forbes MS, Sperelakis N. Ultrastructure of cardiac muscle from dystrophic mice. *Am J Anat* 1972;**134**:271–290.
24. Chidgey M. Desmosomes and diseases: an update. *Histol Histopathol* 2002;**17**:1179–1192.

25. Bierkamp C, McLaughlin KJ, Schwarz H, Huber O, Kemler R. Embryonic heart and skin defects in mice lacking plakoglobin. *Dev Biol* 1996; **180**:780–785.
26. Roncali L, Nico B, Locuratolo N, Bertossi M, Chiddo A. Right ventricular dysplasia: an ultrastructural study. *Eur Heart J* 1989;**10**:D97–D99.
27. Guiraudon CM. Histologic diagnosis of right ventricular dysplasia: a role for electron microscopy? *Eur Heart J* 1989;**10**:D95–D96.
28. Norgett EE, Hatsell SJ, Carvajal-Huerta L, Cabezas JC, Common J, Purkis PE, Whittock N, Leigh IM, Stevens HP, Kelsell DP. Recessive mutation in desmoplakin disrupts desmoplakin-intermediate filament interactions and causes dilated cardiomyopathy, woolly hair and keratoderma. *Hum Mol Genet* 2000;**9**:2761–2766.
29. Kaplan SR, Gard JJ, Protonotarios N, Tsatsopoulou A, Spiliopoulou C, Anastasakis A, Squarcioni CP, McKenna WJ, Thiene G, Basso C, Brousse N, Fontaine G, Saffitz JE. Remodeling of myocyte gap junctions in arrhythmogenic right ventricular cardiomyopathy due to a deletion in plakoglobin (Naxos disease). *Heart Rhythm* 2004; **1**:3–11.
30. Runge MS, Stouffer GA, Sheahan RG, Yamamoto S, Tsyplenkova VG, James TN. Morphological patterns of death by myocytes in arrhythmogenic right ventricular dysplasia. *Am J Med Sci* 2000;**320**:310–319.
31. Valente M, Calabrese F, Thiene G, Angelini A, Basso C, Nava A, Rossi L. *In vivo* evidence of apoptosis in arrhythmogenic right ventricular cardiomyopathy. *Am J Pathol* 1998;**152**:479–484.
32. Zhurinskky J, Shtutman M, Ben-Ze'ev A. Plakoglobin and β-catenin: protein interaction, regulation and biological roles. *J Cell Sci* 2000;**113**:3127–3139.
33. Blankenship DC, Hug G, Balko G, van der Bel-Kann J, Coith RL Jr, Engel PJ. Hemodynamic and myocyte mitochondrial ultrastructural abnormalities in arrhythmogenic right ventricular dysplasia. *Am Heart J* 1993;**126**:989–995.
34. Masani F, Aizawa Y, Izumi T, Shibata A. An ultrastructural study on arrhythmogenic right ventricular dysplasia with special reference to lipid droplets. *Heart Vessels Suppl* 1990;**5**:55–58.
35. Sekiguchi M, Kinoshita O, Yazaki Y. Ultrastructural observations. In: Nava A, Rossi L, Thiene G, eds. *Arrhythmogenic Right Ventricular Cardiomyopathy/Dysplasia*. Amsterdam: Elsevier Science B.V, 1997. p139–144.
36. d'Amati G, di Gioia CR, Giordano C, Gallo P. Myocyte transdifferentiation: a possible pathogenetic mechanism for arrhythmogenic right ventricular cardiomyopathy. *Arch Pathol Lab Med* 2000;**124**:287–290.
37. Thiene G, Corrado D, Basso C. Cardiomyopathies: is it time for molecular classification? *Eur Heart J* 2004;**25**:1772–1775.